The optical detector systems of UVES, the echelle spectrograph for the UT2 Kueyen Telescope at the ESO Paranal Observatory

Reinhold J. Dorn, James W. Beletic, Cyril Cavadore and J.L. Lizon

European Southern Observatory
Instrumentation Division
Karl-Schwarzschild-Str.2, D-85748 Garching, Germany

ABSTRACT

This paper presents the design, construction and performance parameters for the optical detector systems for UVES [1], the echelle spectrograph for the UT2 Kueyen Telescope at the ESO Paranal. A general overview at system level with a description of the individual components is also given. Emphasis is given on the CCD detectors and their performance. The two arms are equipped with large science CCD detectors, one single chip in the blue arm and a mosaic of two in the red. The blue CCD is a 2K x 4K, 15 µm pixel size thinned EEV CCD-44. The mosaic in the red arm is made of an EEV chip of the same type and an MIT/LL CCID-20 chip (2K x 4K), which features a higher NIR QE and reduced fringing for the redder part of the spectral range. The read noise archived with the CCDs at the telescope is less than 2 electrons for the EEV CCDs and less than 3 electrons for the MIT/LL CCD at a readout speed of 50 kpixel/sec/port. The systems offer a variety of readout modes, binning options and readout speeds up to 625 kilopixel per second per port with linearity variations better than 1% peak to peak at a dark current level of around 0.5 electrons/pixel/hour.

Keywords: CCDs, astronomical instrumentation, CCD controller, spectrograph, CCD system design

1. INTRODUCTION

UVES is a two-arm crossdispersed echelle spectrograph covering the wavelength range 300 - 500 nm (blue) and 420 - 1100 nm (red), with the possibility to use dichroics. The spectral resolution for a 1 arcsec slit is about 40,000. The maximum resolution that can be attained with still adequate sampling, using a narrow slit, is about 110,000 in the red and 80,000 in the blue. The dioptric cameras offer fields with a diameter of 43.5 mm (blue) and 87 mm (red) and have external focal planes for easy detector interfacing and upgrading during the life of the instrument.

Figure 1 - UVES instrument during installation at the telescope

The two arms are equipped with CCD detectors, one single EEV CCD-44 (2K x 4K, 15 µm pixel size thinned) in the blue arm and a mosaic of two in the red. The red CCD mosaic is made of an EEV chip of the same type and the MIT/LL CCID-20 chip. Each arm has two crossdisperser gratings working in first order; the order separation is 10 arcsec minimum. Auxiliary devices include the usual calibration lamps, an Iodine absorption cell for high precision radial velocity studies, image slicers, a depolarizer, an image derotator, an Atmospheric Dispersion Compensator and filter wheels. The instrument components are placed inside a passive enclosure, which provides thermal isolation from the environment. The control and CCD electronics are located in temperature controlled cabinets outside the enclosure.

Further author information - E-mail: reinhold.dorn@eso.org

All functions (image slicers, filters, ADC etc.) are permanently on-board and remotely selectable without manual intervention. A continuous flow of liquid nitrogen coolant for the CCDs is supplied by an external vessel with autonomy of at least 2 weeks. Figure 1 shows a picture of the UVES instrument during the installation at the UT2 telescope in Paranal. On the right side of the picture the red arm detector cryostat can be seen mounted to the camera.

2. Detector system level overview and components

The UVES optical detector systems use the ESO standard FIERA CCD controller [2]. The FIERA system with all its components is displayed in Figure 2. The functionality of the system components is as follows:

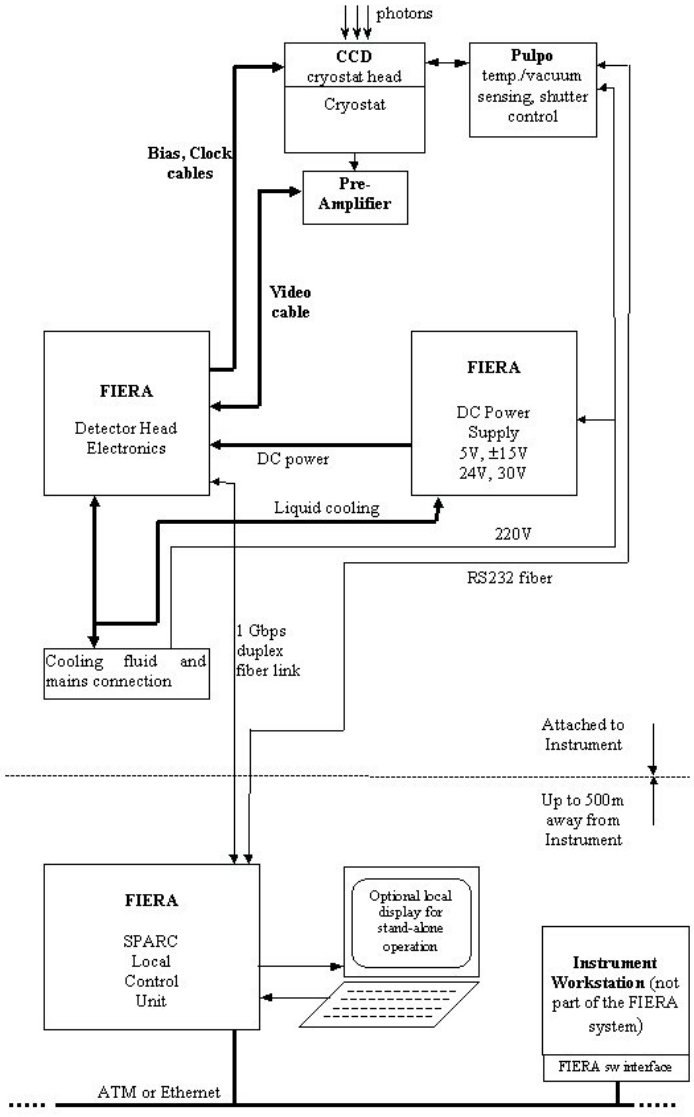

- Cryostat head: Holds the CCD, the CCD temperature control and monitoring circuitry.
- Cryostat: vacuum-isolated reservoir of liquid nitrogen for cooling the CCD to 150-170 K.
- Cryostat Controller for the continuous flow cryostats controls the flow of liquid nitrogen through the Continuous Flow Cryostat, the temperature of the nitrogen exhaust gas, and the temperature of the sorption pumps. The Cryostat Controller can be monitored via a serial interface (RS485 or RS232).
- PULPO micro-controller-based 'house-keeping' unit, that controls the CCD temperature, monitors the cryostat's vacuum, and provides shutter control for a variety of different shutter types. PULPO is connected to the SLCU via a RS232 fiber link.
- Preamplifiers: Amplifies the CCD video signals. Four amplifiers are located in one Preamplifier box. The Preamplifiers have to be located close to the cryostat head's video connectors (max. cable length of the video input cable is 10cm).
- Detector Head Electronics: The detector head electronics provides clock and bias voltages to the CCD, and performs the video signal preprocessing, digitization, and data transmission to the SLCU-rack.
- DC Power Supply: Provides DC-power to the Detector Head Electronics. All power supplies are linear for low-noise operation
- Sparc Local Control Unit (SLCU): The SLCU initiates and controls the CCD operation, i.e. wiping, integration, and readout.

Figure 2 - Schematic overview of the Detector system CCD system

A Sparc-CPU in the SLCU-rack performs the higher level coordination of these operations, whereas a DSP-board functions as a real-time controller. The DSP-board is directly connected to the Detector Head Electronics via a fiber link. Apart from the CCD-control function, the Sparc communicates directly to PULPO for temperature control of the cryostat head and monitoring of the cryostat's vacuum. For stand-alone operation in the laboratory a display and keyboard can be attached. The instrument workstation can be omitted in that case.

- Instrument Workstation: Controls complete instrument. A part of the detector system software runs on the instrument workstation and communicates to the Sparc Local Control Unit.

2.1 FIERA CCD controller System Architecture

The architecture of the FIERA CCD controllers can be described to consist of three major parts in general. For more information on FIERA the reader is referred to the following papers [2,3]. The three parts are:

- A sequencer which generates all necessary signals for the switching of clock lines as well as control signals for the analog preprocessing of the video signal. It usually also includes a slow-speed command interface to a higher-level computer. This interface is used for controller initialization, telemetry (checking of voltages, which are applied, to the CCD), mode control, etc. Implementations of the sequencer with digital signal processors (DSP), transputers, or Gate Arrays are common. The sequencer is usually implemented in a single processor.
- A clock driver module, which employs the sequencer's output signals to switch the CCDs clock voltages between lower and upper rail voltages. In this part we also group the generation of analog bias voltages for the detector. These DC voltages are mainly used to supply the CCDs output amplifier.
- A video module which contains the analog preprocessing of the CCDs video signal and A/D-conversion. A fiber interface is used in many systems to transmit the data galvanically isolated over a high-speed path to the higher-level computer. Figure 3 shows the electronic boards in the detectorhead box and the power supply box in the custom developed housing of the FIERA CCD controller.

Figure 3 - FIERA power supply and detector head box

2.2 CCD Preamplifiers

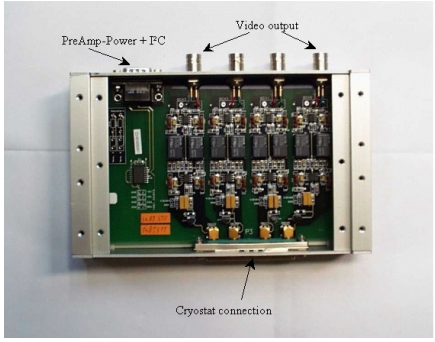

Figure 4 - CCD preamplifier with 4 channels

Because of space constraints the Detector Head Electronics Box can usually not be attached directly to the CCD head. Therefore, FIERA employs a separate Pre-Amplifier box, which boosts the CCDs single-ended video signals, and converts them into a differential signal pair. The Pre Amp is connected to the CCD head video connector with a cable of less than 10-cm length. The amplified and differential video is output to the Detector Head Electronics Box using Twix-cables with a maximum length of 2m. One Pre Amplifier-PCB provides four video channels with each one independently controllable gain switch. Each gain switch can be adjusted to any of four settings. The gains are remotely controlled by software via an I²C-bus from the video board in the detector head electronics.

2.3 PULPO temperature controller

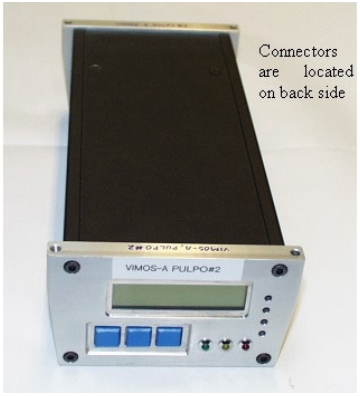

Figure 5 - PULPO housekeeping box

PULPO [4] is a versatile micro-controller based unit for housekeeping purposes. It provides the following capabilities in one box. Shutter control for a variety of different shutter types. Based on status signals, which are generated by the shutter, PULPO can measure the exact time difference between open and close status. The resulting exposure time is then communicated to the SLCU. CCD temperature monitoring and control. Up to seven PT100 temperature sensors can be monitored by PULPO. An output with 1A max. current can be used to control one temperature, e.g. of a CCD and monitoring the temperature of the electronic housings. Vacuum monitoring based on a 0-10V output from a vacuum gauge. A user interface based on a LCD-panel and a small keypad. A serial interface for connection to the SLCU. A simple protocol is used to read monitored sensor outputs, set desired values, and control the shutter.

2.4 Water Cooling System and Housings

At the VLT a requirement for all electronics mounted in the telescope dome is that all surface temperatures of any housings should not be higher than 1 °C compared to the ambient temperature. For the FIERA CCD Controller therefore an active cooled housing has been developed to provide good electromagnetic shielding and to carry away the heat produced by the electronic boards. The FIERA active water-cooling system acts like a typical closed loop liquid cooling system. In a typical closed loop air cooling system cool water is supplied to the heat exchanger and (filtered) air is circulated between an electronic enclosure and a heat exchanger which then transfers the heat to the water flowing through the tubes. Our heat exchanger is placed inside the enclosure with cooled exit air blown directly through the FIERA boards and power supplies. This system permits closed loop air-cooling and prevents entry of contaminated intrusion air. Heat exchangers require some temperature difference between liquid and air entering the heat exchanger. In the VLT environment the incoming water temperature of the heat exchanger is regulated to be always 8 °C below the ambient temperature. In order to dissipate the entire thermal energy produced, the thermal performance of the FIERA heat exchanger was specified as follows. To rate the thermal performance (TP) of our heat exchanger the following equation was applied:

$$\mathrm{TP\ [Watts/^\circ C]} = \frac{Q}{T_{\mathrm{air\ in}} - T_{\mathrm{water\ in}}} = \frac{\text{Thermal energy produced by the boards or power supplies}}{\text{Air temperature into HX} \quad \text{- Watertemperature into HX}}$$

Figure 6 shows the FIERA heat exchanger mounted on the rack unit. The heat exchanger is equipped with 4 slim-line low noise fans to blow air through the complete area of the electronic boards. The fans are wired in parallel and operated with 24V DC voltages. The operating temperature range is from –10 C to +70 C. Additional a temperature sensor (PT100) is mounted on the rack on a cooling profile.
This sensor monitors the air temperature inside the box and will give the reference value for the flow control unit. It will dissipate 200 Watts as a maximum value with a fully equipped FIERA detector head (11slots) or power supply box. With an initial temperature difference of 8 C, the heat exchanger must have a minimum thermal performance of 25 Watts/°C. The result from the custom made heat exchanger is a little bit better and has a TP of 27 Watts/°C. If the incoming water temperature is constant at 10 C, the incoming air will stabilize at 17.4 C. The FIERA housings are also equipped with an overheat protection, which shuts the system down if the temperature in the boxes exceeds 40 °C. This prevents any damage to the electronic boards if there are problems with the external cooling system. The system is not software controlled and therefore is completely independent from the control software. Nevertheless, during operation the temperature in the boxes is monitored and an alarm will be given if the temperature rises too high before the system shuts down.

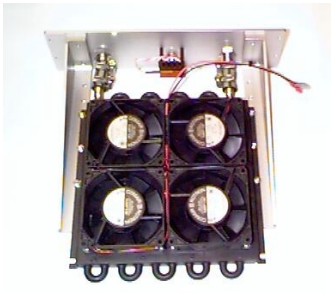

Figure 6 - FIERA water-cooling unit

2.5 CCD head and interface printed circuit boards

The CCDs for the red and blue arm systems are implemented in an ESO standard CCD head, which provides the mounting of the CCDs and the attachment to the cold-finger of the CFC cryostat. To operate the CCDs a special multi-layer, flex-rigid inter-PCB for a single EEV chip and the red mosaic, consisting of an EEV and MIT/LL chip, has been designed. On this PCB the passive filters for the CCD clock phases and the capacitors for filtering the bias voltages have been implemented. For the EEV CCDs socket boards with a ZIF socket have been design, which then connect to the interPCB. The video-outputs run over special shielded coaxial cables to CCD head vacuum connectors. Figure 7 shows the interPCB for the UVES red mosaic and figure 8 the ZIF socket board for the EEV CCD and the invar mounting plate for the mosaic.

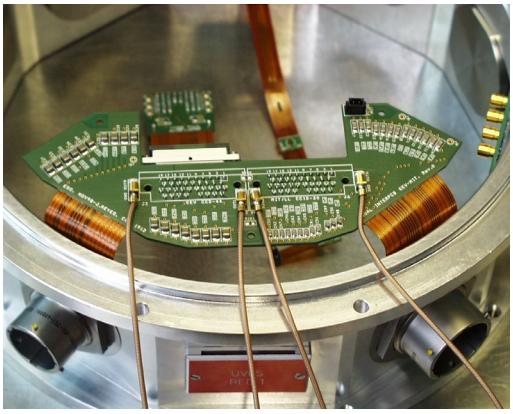

Figure 7 - UVES red interPCB

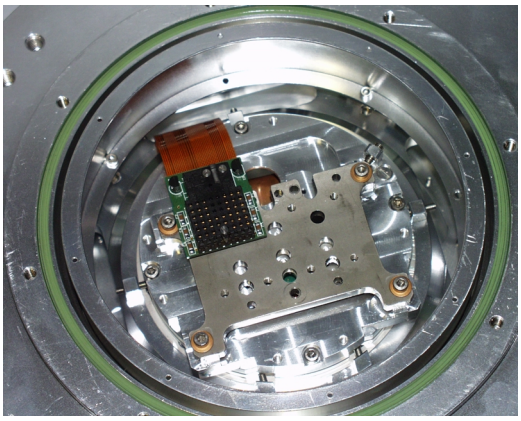

Figure 8 - ZIF socket and invar mounting plate

2.6 CCD - Continuous Flow Cryostat

CCDs used in astronomy must be cooled from 140 to 160 K to reduce dark current to a negligible level. For this reason, the CCD detectors are mounted in vacuum dewars with cooling provided by liquid nitrogen (77 K). In addition to keeping the CCD cold, the dewar also holds the CCD in a very rigid position, with motion of less than 3 microns as the telescope points to different positions in the sky. Some large instruments or instruments fitted with optical fibers simply rest on the Nasmyth platform and do not move relative to the telescope building. UVES is the first instrument of this type and, being a high-resolution spectrograph, it is very sensitive to any type of disturbance, especially thermal variations. For this reason the complete instrument, including the two detector systems, is surrounded by a thermal and light tight enclosure. It would be a major source of disturbance if it were necessary to open the thermal enclosure to refill the detector cryostats every day. Therefore, for UVES, and other Nasmyth and coudé instruments, a continuous-flow cryostat has been developed [5]. This cryostat is based on a continuous circulation of coolant supplied from a delocalised re-serve of liquid nitrogen. This system uses a large tank of liquid nitrogen so that the cooling operates autonomously for relatively long periods between replacement of the nitrogen reservoir. Another advantage of the continuous-flow cryostat is that it only occupies a small volume at the instrument. Figure 9 shows the compactness of the continuous-flow cryostat relative to the detector-head tank. The head is then mounted directly to the UVES cameras.

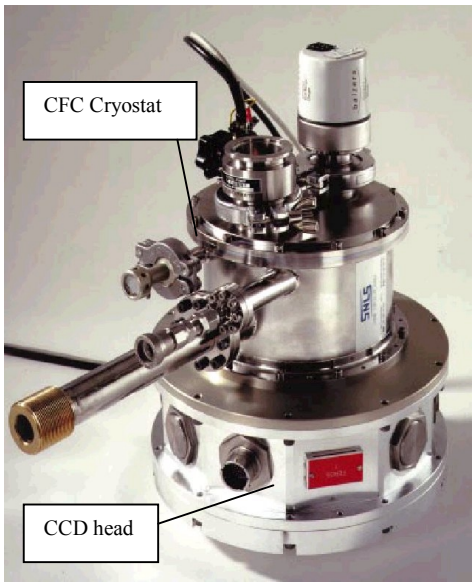

Figure 9 - Continuous-flow cryostat and CCD head

3.0 CCD properties and performance

UVES used two different kinds of CCDs for the science detector systems. The EEV CCD-44-82 and the MIT/LL CCID-20. For the MIT devices, ESO is part of the University of Hawaii consortium. These devices have a better near infrared quantum efficiency and will be used mainly for instruments demanding higher sensitivity in this spectrum domain. Up to now, the Optical Detector Team (ODT) has implemented one of these devices into the red arm of the UVES spectrograph. Both devices have 2 readout ports. The CCDs can be operated either in dual readout mode using two ports, or single port readout. Binning along the X and Y direction is possible using any kind of binning factor provided that the scene is not over-saturated. For the EEV a fast wiping of the device can be achieved by using a dump gate close to the serial register. Both CCDs are backside, full frame and frame transfer capable, 2k x 4k, 15 µm pixel size with a readout speed up to 1 million pixel per second. The flatness of all devices is typically around ±10 µm peak to peak. The differences are mainly the quantum efficiency (QE) and the full well capacity of the devices. The EEV CCDs have a full well capacity of 225 000 electrons with good QE especially in the UV whereas the MIT/LL CCD has full well capacity of around 130 000 electrons and excellent QE in the near -IR. Figures 10 and 11 show pictures of two the devices used for the UVES spectrograph. Figure 12 shows the CCD installed in the red CCD head.

Figure 10 - EEV CCD-44-82(UVES blue and red)

Figure 11 - MIT/LL CCID-20 (UVES red)

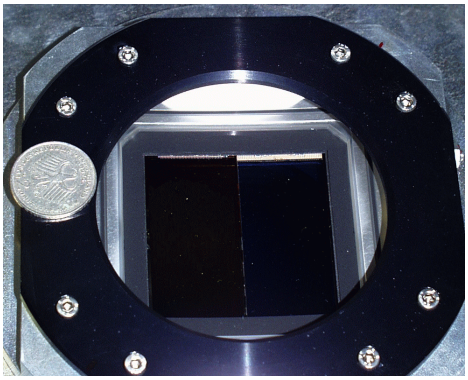

Figure 12 - UVES RED CCDs installed in the CCD head (EEV on the left, MIT to the right)

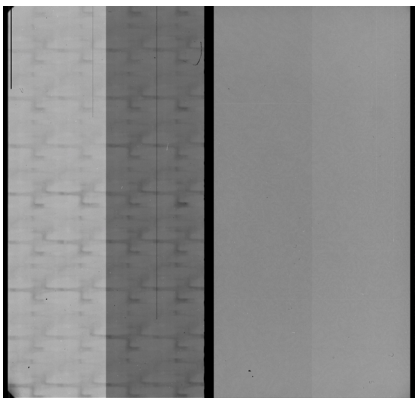

Figure 13 : UVES red flat field at 650 nm (4 port image , MIT/LL right, EEV left)

3.1 Image setup and readout modes

The UVES blue science detector is a single EEV CCD-44. An optical field size 30.7 x 30.7 mm is required and therefore only a window of the CCD (2048 x 3000 pixels) is used for the blue arm. The first 551 lines and the last 551 horizontal; lines are dumped and only the inner 3000 lines are read out. There are 50 physical prescan pixels for each output port of the CCD. The red system is a mosaic of one MIT and one EEV CCD. The optical field required is 61.4 x 61.4 mm and therefore all pixels in both devices are read out. The MIT has only 10 prescan pixels in the serial register and therefore to get the same images size as the EEV since the CCDs are clocked in parallel 40 "virtual pixel" pixels are produced prior to the physical prescan pixels for the MIT/LL. Note that these pixels do not contain any useful data. Figure 14 and 15 show the image setup

for both systems. Various readout modes have been programmed, raging from pixel speeds of 50 kilopixel per second to 625 kilopixel per second. All these modes are technically available but three modes have been chosen for regular science operation at the telescope. These modes were calibrated during the installation at the telescope in September 1999 and the following tables 1,2 and 3 give a summary of the modes available and the performance of the CCDs in terms of gain, readout noise, dark current, linearity and charge transfer efficiency.

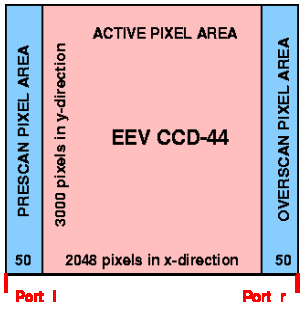

Figure 14 - Images setup for the blue CCD

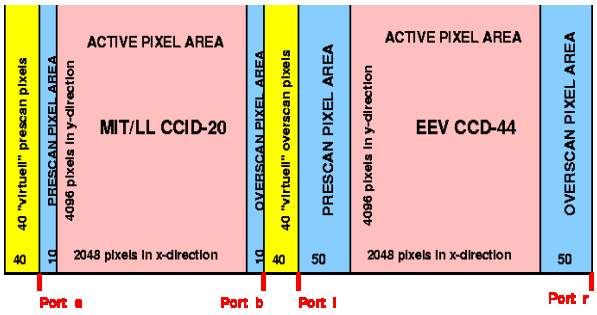

Figure 15 - Image setup for the red CCDs. Note: not drawn to scale

3.2 Performance of the CCDs

Following is a summary on the performance of the UVES CCDs measured in September 1999 at the telescope at the Paranal Observatory. For the EEV CCDs, readout noise values were measured less than 2 electrons at 50 kps. For the MIT/LL CCD, the noise at the same speed is about 1 electron higher. Since this chip was the first device of its kind that the ODT worked with, it was not optimized to the full extent. The linearity values are excellent for all devices and readout speeds and good CTE was measured also at low level flat field exposures.

3.2.1 Performance of the UVES Blue Arm CCD

Device :EEV CCD-44-82 nicknamed "MARLENE" **CCD operating temperature :** - 118 °C

Read out	*units*	225 kps / 1x1 binning / low gain / one port	225 kps / 1x2 binning / low gain / one port	50 kps / 2x2 binning / high gain / one port	50 kps / 2x3 binning / high gain / one port
Conversion factor	e^- / *ADU*	2.04	2.04	0.58	0.58
Readout noise	e^-	3.90	3.90	2.14	2.14
Dark current (system up and dark 24 h)	e^- / *pix* / *h*	-	-	1.0 (1st 1 h dark) 0.5 (2nd 1 h dark) 0.4 (12th 1 h dark)	1.0 (1st 1 h dark) 0.5 (2nd 1 h dark) 0.4 (12th 1 h dark)
Linearity	*% p-p*	+ 0.57 / - 0.55	+ 0.57 / - 0.55	+ 0.42 / - 0.34	+ 0.42 / - 0.34
Cosmic ray hit rate	*hits* / cm^2 / *h*	114	114	100	100
CTE (X)	-	0.999999 @ 10^5 e^-	0.999999 @ 10^5 e^-	0.999997 @ 3 x 10^4 e^- 0.999980 @ 3 x 10^3 e^-	0.999997 @ 3 x 10^3 e^- 0.999980 @ 3 x 10^3 e^-

Table 1 - Performance of the UVES Blue Arm CCD Marlene

3.2.2 Performance of the UVES Red Arm CCDs

Device : EEV CCD-44-82 nicknamed "STING" **CCD operating temperature :** - 118 °C

Read out	*units*	225 kps / 1x1 binning / low gain / one port	225 kps / 1x2 binning / low gain / one port	50 kps / 2x2 binning / high gain / one port	50 kps / 2x3 binning / high gain / one port
Conversion factor	e^- / *ADU*	1.59	1.59	0.52	0.52
Readout noise	e^-	3.42	3.42	1.92	1.92
Dark current (system up and dark 24 h)	e^- / *pix* / *h*	-	-	0.4	0.4
Linearity	*% p-p*	+ 0.42 / - 0.48	+ 0.42 / - 0.48	+ 0.15 / - 0.12	+ 0.15 / - 0.12
Cosmic ray hit rate	*hits* / cm^2 / *h*	112	112	113	113
CTE (X)	-	0.999998 @ 6 x 10^4 e^-	0.999998 @ 6 x 10^4 e^-	0.999890 @ 2 x 10^2 e^- 0.999997 @ 3 x 10^4 e^-	0.999890 @ 2 x 10^2 e^- 0.999997 @ 3 x 10^4 e^-

Table 2 - Performance of the UVES Red Arm CCD Sting

Device : MIT CCID-20 nicknamed "NIGEL" **CCD operating temperature :** - 118 °C

Read out	*units*	225 kps / 1x1 binning / low gain / one port	225 kps / 1x2 binning / low gain / one port	50 kps / 2x2 binning / high gain / one port	50 kps / 2x3 binning / high gain / one port
Conversion factor	e^- / ADU	1.48	1.48	0.57	0.57
Readout noise	e^-	3.69	3.69	2.87	2.87
Dark current (system up and dark 24 h)	$e^- / pix / h$	-	-	0.6	0.6
Linearity	*% p-p*	+ 0.10 / - 0.10	+ 0.10 / - 0.10	+ 0.03 / - 0.03	+ 0.03 / - 0.03
Cosmic ray hit rate (events 30 e^-)	$hits / cm^2 / h$	108	108	102	102
CTE (X)	-	0.999998 @ 8 x 10^4 e^-	0.999998 @ 8 x 10^4 e^-	-	-

Table 3 - Performance of the UVES Red Arm CCD Nigel

3.3 Quantum efficiency and cosmetic quality of the CCD detectors

UVES as a spectrograph requires very good CCDs in terms of cosmetic quality, QE and readout noise. All three CCD were underwent extensive tests at the ESO CCD testbench [6] to measure all features before installing the CCDs in the UVES systems. Following we present the results obtained there. The different kind of defects, which degrade the cosmetic quality of the device, can be split in three parts:

- Defects visible in the bias images (mainly hot pixels)
- Defects visible with a low light level flat field (traps)
- Defects visible in the median stack of five 1h exposed dark frame (mainly over-saturated hot pixels, trails).
  A defect pixel is a pixel value above or below 5 sigmas from the mean of the neighborhood pixels.

For the UVES blue EEV CCD-44, "Marlene", only a very view cosmetic defect are visible, an almost perfect device. On a low level flat field there is only one small trap with 52 affected pixels. On a bias Image (0 seconds dark exposure) 104 pixels above 5 sigma and for a long exposure dark image (4 exposures of 3.600 seconds), 355 pixels above 5 sigma. For the UVES red EEV CCD-44, "STING", the defects are mainly hot pixel trails seen in long dark exposures. 572 pixels were found above 5 sigma. The EEV CCD devices are made of 1024x512 blocks, and the area boundaries show sometime a 1-2% QE variation over 1 row/column due to photolithography stepper mismatches. These small defects flat field out perfectly. Trap defects are a determining factor for assigning devices to certain applications. These kinds of defects cannot be suppressed because they are created during chip fabrication, and are not temperature dependent. Finally, the amount of the "defects" induced by cosmic rays should not be more than what is caused by natural radioactivity. The CCD package and the head of the detector do not add additional hits. This value is typically measured between 1 and 1.5 event/min/cm^2.

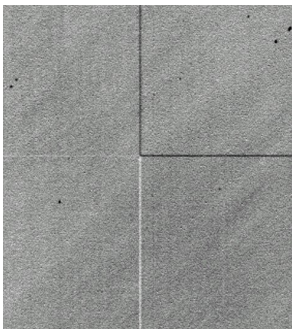

Figure 16 - Effect of block Stitching between 1K x 512 areas

The MIT/LL CCID-20 "NIGEL" also has good cosmetic quality. The only bigger problem with the MIT/LL device for scientific use are two partially blocked columns (one of them very short) and one very bright column. The bright column is caused by a single hot pixel in the first imaging column on the left -amplifier side of the CCD.

On a low-level flat field one hot column and 3 traps were detected. On a bias image 1520 pixels are above 5σ with 2 hot columns and on long exposure dark images (5 exp. of 3600 sec each), 2432 pixels are above 5σ, one defect column and very hot pixel + trail and 4 traps are visible. Brickwall pattern is strongly visible at short wavelengths but flat fields out very easily. For detailed information the reader is referred to the ODT webpages for the UVES CCD system: http://www.eso.org/projects/odt/Uves/uves.html. Figure 17 shows the quantum efficiency of the 3 CCDs.

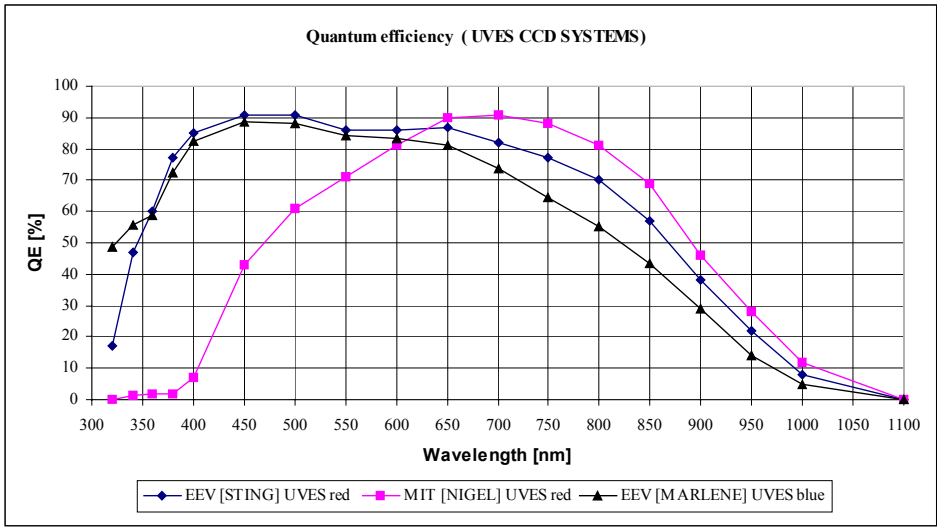

Figure 17 - Quantum efficiency of the EEVs and MIT/LL CCID-20 (W7C2) CCDs. The MIT QE tops out at over 91% and gives a good near infrared QE with over 28 % at 950 nm.

Fringing- Photo Response Non Uniformity (PRNU) for the EEV devices

Fringing is an issue especially for a spectrograph making images harder to flat field out. The ODT has measured this effect with the UVES CCDs [7]. A parameter called PRNU (Photo-response non-uniformity) gives the QE uniformity across the chip. The near IR PRNU depends on the fringing effect. This effect is related to the CCD thinning, its thickness, the IR penetration depths into the silicon and to the aperture of the incoming beam and the bandwidth of the incoming light. The more this beam is open, the less the fringing is visible. In the blue part of the spectrum, the PRNU also increases due to a pattern related to the backside p+ implementation laser annealing. The images in figure 18 show qualitatively these effects for the EEV devices.

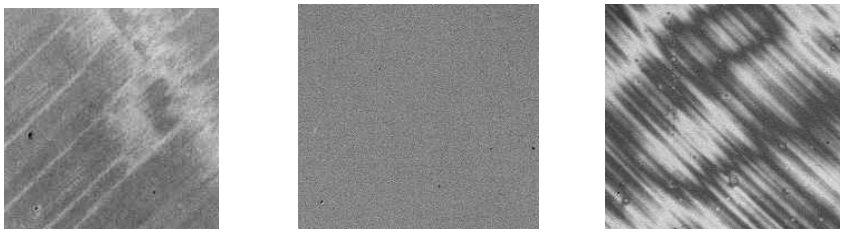

Figure 18 - Flat fields from the same area at different wavelengths, 5nm bandwidth, left 320nm, middle 650nm, right 950nm, F/2 beam. 300x300 pixels, 15 μm thick device

Between 400 nm and 850 nm, the PRNU is very low and almost photon-noise limited (the stitching pattern is visible). The PRNU is measured using a dust-free area and taking 10% and 90% of the computed histogram as deviation figures. Below 400 nm, a diamond pattern is visible. This can be flat fielded out easily, if the CCD temperature is stable within 2-3 degrees. Measurements how stable the diamond pattern with changes to the CCD temperature is, show a 1.25 % p-p change in PRNU within a variation of 20 degrees (170 K - 150 K). Concerning IR fringing, this is strongly dependent on the bandwidth and the wavelength of the incoming light. Figures 18b and 18c show the PRNU at a bandwidth of 2 and 7 nm over a wavelength range of 750 to 950 nm. Obviously the EEV devices are strongly sensitive to fringing effects, providing a high spatial frequency pattern difficult to cancel out. For a spectrograph like UVES, the local bandwidth is extremely low and thus fringing becomes a bigger problem.

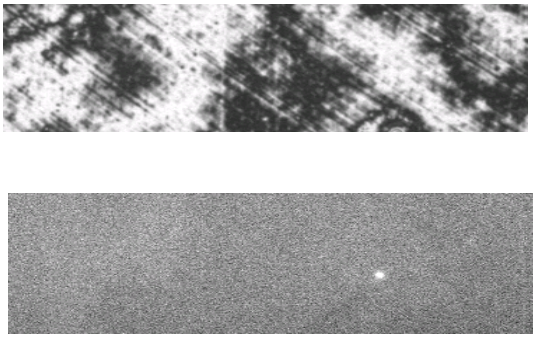

Figure 18b - Top 950nm, 2nm bandwidth, bottom same wavelength, 7nmbandwidth

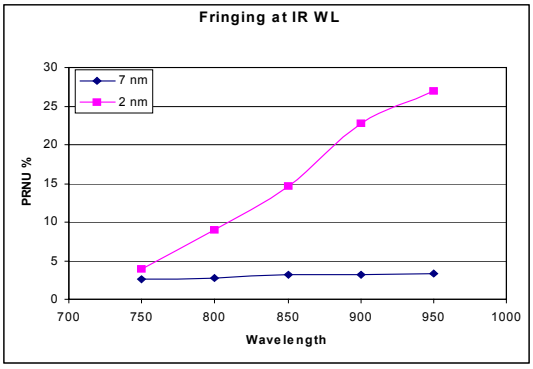

Figure 18c - PRNU versus bandwidth and wavelength

Fringing / Photo-response non-uniformity for the MIT device

Generally the same effect applies to the MIT device. Nevertheless in the IR band, the CCD should be less affected because it is slightly thicker then EEV devices (20 µm instead of 15 µm). Measurements showed the same amount of PRNU for both devices. However, the MIT device has a lower spatial frequency of fringing, meaning that the surface of the CCD is flatter and its parallelism is improved (see fig19).

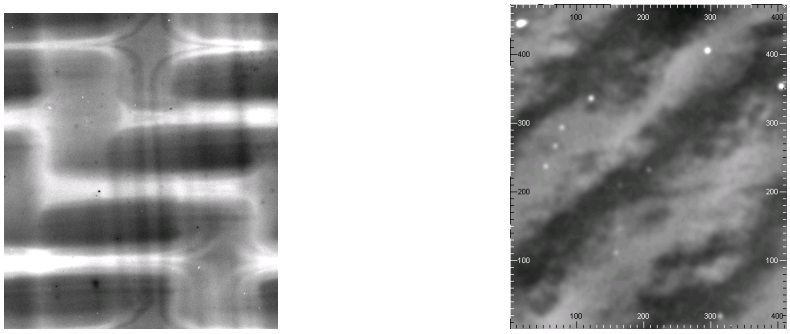

Figure 19 - Typical image with strong brick-wall pattern visible at 350 nm (bandwidth=5nm), 400x400 pixels area wide (right image) and typical image of NIR fringing pattern (left image) visible at 850 nm (bandwidth=5nm).

The higher PRNU (up to 40%) of the MIT/LL device at a wavelength of 300 to 400nm are related to the backside laser annealing process. The image at 350 nm shows the typical brick-wall pattern. For upcoming MIT/LL devices the uniformity of the laser annealing process was enhanced and the brick-wall patterns was reduced. Figure 20 shows a comparison of the PRNU measured for the MIT/LL CCID-20 and EEV–44 devices with a bandwidth for the incoming beam of 5 nm.

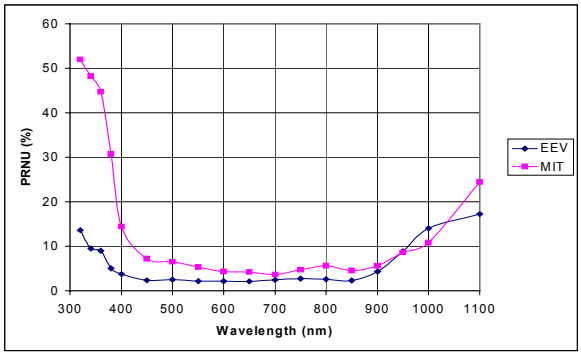

Figure 20 – Comparison of PRNU (MIT/LL and EEV devices) with a 5nm incoming bandwidth beam at F/3

Remanence effects- residual image

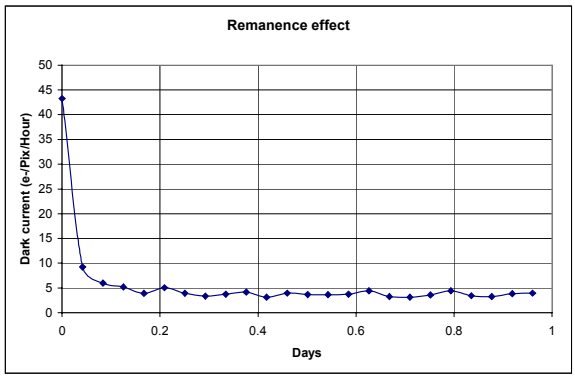

Remanence effects may occur if a flat field (Mean>10000e-) is taken prior to the dark frame and after powering up the system. The resulting effect resembles an increase of dark current, especially at temperatures lower than 180K. The ODT is currently investigating a way to cure this problem by applying a special wiping sequence (with different parallel voltages). Figure 21 shows a set of 24 dark frames exposed each one-hour (CCD operating temperature at 160K). This set was taken after the CCD was exposed to the ambient light. It requires four 1 hour dark frames to eliminate the residual image and to reach the actual dark current value (about 3 to 5 e-/pix/hour) at that temperature. The UVES CCDs are operated at -118 C and a dark current of ~ 0.6 e^-/pix/h is measured under normal operation.

Figure 21- Remanence effect

Nevertheless this value is only reached after the system is powered on for at least 24 h. Higher values up to 3 electrons per pixel per hour are measured directly after powering up the system. This is caused by the remanence effect explain above and occurs on the MIT and EEV CCDs. For now we have implemented a continuous periodic wiping for the UVES CCDs at the telescope. This means that the chips get wiped periodically, every 10 seconds, when the system does not take an exposure.

Figure 22a - 2048x512 pixel subframe of the EEV devices, one hour exposure dark frame, just after a flat field, the dark current is 43e-/pixel/hour and the "dark current" is related to the"blue diamond" pattern.

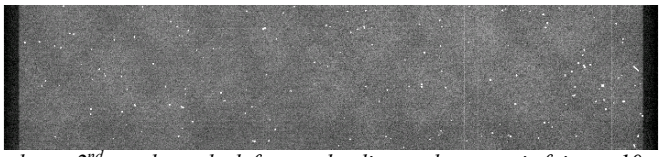

Figure22b - Same frame as above, 2nd one hour dark frame, the diamond pattern is fainter, 10e-/pixel/hour of dark-current. Overscan/Prescan area is visible.

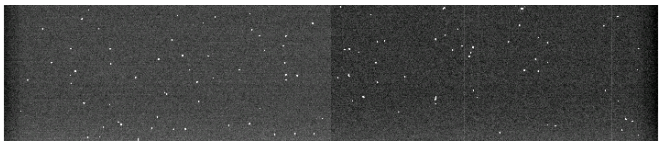

Figure 22c - Same frame as above, 28th one hour dark frame, dark current has reached its minimum value (4e-/pix/hour).

3.5 Flatness Measurements for the UVES CCDs.

One important opto-mechanical requirement for the UVES CCDs is the peak-valley flatness, which is the distance of the two planes, parallel to the reference flange, between which the sensitive surface of the chip or mosaic is contained. This applies to optical field size only. For the mosaic also the gap, the width of optically inactive area between two chips should be as small a possible. The gap runs parallel to the readout detector by 90°. For the UVES red CCDs the gap is around 1 mm between the CCDs. One full order is lost in the gap. We have measured under cooled down conditions the flatness of the CCDs and the flatness with respect to the window backside of the cryostat window. The following results were obtained. Figure 23 shows the topography of "MARLENE" with respect to the window backside at - 120°C (p-v = 0.0320 mm). The chip itself has a flatness of p-v=0.0017 mm at - 120°C. Figure 24 shows the topography of "NIGEL" and "STING", the

UVES red CCDs with respect to the window backside at - 120°C (p-v = 0.0626 mm). The chips themselves have a flatness of p-v of 0.0251 mm at 120 °C [8].

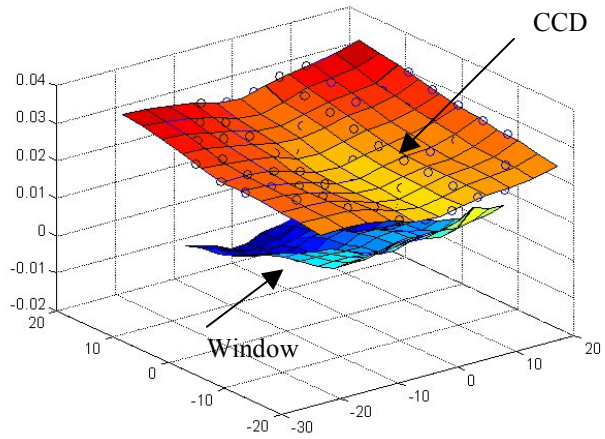

Figure 23 - The topography of "MARLENE" with respect to the window backside at - 120 °C

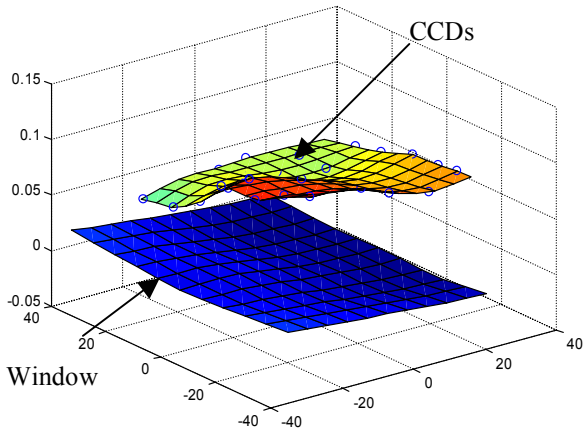

Figure 24 - Topography of "NIGEL" and "STING" with respect to the window backside at - 120 °C

4. Conclusion

The CCDs detector systems for the UVES spectrograph have been performing without any problems since September 1999 at the UT2 telescope at the VLT site in Paranal. The systems incorporate excellent "new generation" CCD devices. The CCDs are very high-end performance devices due to very good quantum efficiency (optimized for U, B and V bands). Fast readout is possible. They have low noise and almost no cosmetic defects. The single MIT device is also extremely promising in term of noise and speed, but the noise still needs to be improved by the ESO ODT to reach the lowest noise possible. Combined with the new developed FIERA CCD controller, these systems contribute to the state of the art instruments already installed at Paranal. The success of these detector systems was only possible due to the excellent work of all people in the Optical Detector Team at ESO.

References

[1] H. Dekker, S. D'Odorico, A. Kaufer and H. Kotzlowski, "Design, construction, and operation at the telescope of UVES: the Echelle spectrograph for the UT2 Kueyen Telescope at the ESO Paranal Observatory", proc. SPIE 4008 (in print), 2000.

[2] J.W. Beletic, R. Gerdes and R C. DuVarney, FIERA: "ESO's new generation CCD controller", Astrophysics and space Library, Optical Detector for astronomy, James Beletic, Paola Amico (ed.), Kluwer Academic Publishers.

[3] J Beletic, R. Gerdes and J. Zipperer, 1996 "A DSP-based solution to remote control of detector head electronics for scientific CCD systems", DSP-96, Munich.

[4] Haddad, N. and P. Sinclaire (1997), "PULPO: Temperature, vacuum, shutter, LN2 level, all in one box", ESO Workshop on Optical Detectors forAstronomy, J. Beletic and P. Amico (ed.), Kluwer Academic Publishers.

[5] J.L Lizon,“ New cryostats for scientific CCD systems in the VLT era”, The ESO messenger, No. 88, pp.6-7,1997.

[6] ESO's new CCD testbench, p95, Astrophysics and space Library, Optical Detector for astronomy, James Beletic, Paola Amico (ed.), Kluwer Academic Publishers.

[7] Cyril Cavadore, Reinhold J. Dorn and James W. Belectic , “Charge Coupled Devices at the European Southern Observatory - Performance and results” , in the proceedings of the "ESO workshop on Optical Detectors for Astromony, Garching, September 1999" - P. Amico & J.W. Beletic Eds. Kluwer Academic Publishers.

[8] Stephan Stroebele, " A new machine for planitary measurements of CCDs and mosaics of CCDs", in Optical Detectors for Astronomy II "State -of -the-art at the turn of the Millennium", P. Amico & J.W. Beletic Eds. Kluwer Academic Publishers.